ARTICLE

Check for updates

Strong conformable structure via tension activated kirigami

Tom Corrigan [1✉], Patrick Fleming[1], Charlie Eldredge[1] & Delony Langer-Anderson[1]

Kirigami, the art of cutting and folding sheets, provides a way to deploy three-dimensional shapes from flat material. Known for centuries by artists and the subject of recent research, practical application of kirigami is limited by the complexity of the folding step. Recently, a kirigami pattern based on staggered slits has been used for expanded metal gratings and packaging material, having the practical advantage of deploying with simple tension rather than complex folding. Here, we introduce a tension activated kirigami pattern that drives flat material into rows of vertical, accordion-like, folded walls. This array of walls has a stiffness and strength comparable to a full honeycomb core, yet it self-deploys under tension. The structure is also conformable, allowing it to wrap around objects. These attributes enable a step forward for low-cost structural panels and a sustainable alternative to plastic cushion wrap.

[1] 3M Company, 3M Center, St. Paul, MN 55144, USA. ✉email: Corrigan@mmm.com

The art of creating three-dimensional structures from flat sheets of material has captured the imagination and creativity of people for centuries. Origami, or the folding of sheets, has been used to turn continuous flat materials into complex shapes[1–3]. Origami approaches have been used to create durable, adaptable, bi-stable and inflatable structures[4–6]. A diversity of robotic systems have been built with origami components for actuation or locomotion[7]. Very strong origami structures have also been studied, such as the Miura-Ori pattern[8] and those made with curved-crease folding approaches[9,10]. Kirigami, which involves both cutting and folding, increases the design space and has been widely studied[11–15]. One area of study seeks to increase the conformability of flat sheets or controls their expanded shape by adding slits[16–22]. Much of the work in the realms of kirigami and origami, true to their ancient artforms, involves the controlled folding of flat material. This folding process can be performed by actuators[23,24], by machines[25] or by hand. We find that the folding process can be tedious and inconsistent, creating a potential impediment to broader adoption of kirigami. To bypass the folding process, we have investigated kirigami patterns that deploy from their flat state into their expanded state when tension is applied. The most basic of these Tension Activated Kirigami (TAK) patterns, the single slit, has been widely studied[26,27] and used in a solar tracker[28] and with non-straight slits as a shoe grip[29]. Two applications particularly motivated our investigation into TAK patterns: finding an efficient replacement for honeycomb cores and developing an improved cushioning wrap.

The advantages of honeycomb structures have been widely discussed[30]. Learning from naturally occurring structures in beehives and cork trees, honeycombs are widely used today when a strong, stiff structure is required with minimal weight[31,32]. Researchers have developed mechanical metamaterials that exceed the performance of the honeycomb structure[33], but we use honeycomb as our basis of comparison because of its ubiquity[34]. Today the cores for honeycomb panels are made through a variety of processes taking multiple steps[34,35]. We propose that the creation of cores using self-deploying TAK sheets could offer multiple benefits over current solutions. Three such benefits include lower cost, simplified manufacturing processes, and the creation of field deployable structures where the core is stored flat until the structure is assembled.

TAK structures can also be used, without top and bottom layers, as a protective wrap for objects during storage or shipment. The pattern can be cut into a sheet material such as paper and occupies minimal space until needed. When tension is applied to the material it will deploy to occupy more volume and have some conformability to wrap around oddly shaped objects. The expanded material can absorb energy to protect the items it is wrapped around.

We introduce the Folding-Wall TAK as a useful class of kirigami pattern that expands to produce significant wall structures that are orthogonal to the original plane of the flat material. We show that these expanded Folding-Wall TAK structures are stronger, more voluminous, and can interlock with themselves, all improvements over the basic patterns most widely in use today. As a basis of comparison, we review two configurations of the single slit TAK pattern[11,26–29] and then introduce the Folding-Wall TAK pattern. We describe the deployment mechanics along with experimental results showing the stiffness and strength of the Folding-Wall TAK structure compared to single-slit TAK structures and a constructed honeycomb core of the same material. We also investigate the energy absorbing and volume expansion capability of the Folding-Wall TAK structure compared to single-slit TAK structures in the same material, where we find that it interlocks with itself when multiple layers are wound around themselves or an object, allowing it to stay in place without tape, adhesive, or string. Additionally, modifications to the pattern and materials can enhance the volumetric expansion and the interlocking strength[36].

Results and discussion

Tension Activated Kirigami patterns can be used to expand materials into three-dimensional shapes when tension is applied. The most well-known TAK pattern is the single-slit pattern (Fig. 1a). Straight slits are cut in offset columns with a distance between columns of H, an uncut gap between slits of W, and an overlap distance of L between adjacent slits. When tension is applied along axis T, the slits open and the material buckles forming a 3D structure. Figure 1b shows each column of the pattern buckling the same direction creating a parallel deployed state (Supplementary Movie 1). Figure 1c shows an alternating configuration where adjacent columns buckle in opposite directions (Supplementary Movie 2). We found that materials deployed with an alternating configuration have lower initial stiffness with an interesting higher stiffness and strength after significant strain compared to the parallel configuration. One sheet of material can have some parallel and some alternating columns when deployed. It is also possible to have one column change from parallel to alternating, we call this an inversion. In this study we took care to avoid inversions which generally reduce the strength of the deployed material. The single-slit patterns have surfaces that rotate out of plane, but the rotation of those surfaces is limited.

We developed the Folding-Wall TAK family to produce stronger deployed structures with surfaces that rotate fully orthogonal to the original plane of the sheet. The planar form of the pattern is shown in Fig. 2a along with the primary tension axis T. Figure 2b shows the structure formed when that pattern is cut into kraft paper and tension is applied along the tension axis. We find that the Folding-Wall TAK deploys quickly into the honeycomb pattern visible in Fig. 2b when tension is applied (Supplementary Movie 3). Additional tension causes the hexagonal regions to narrow and elongate but the total
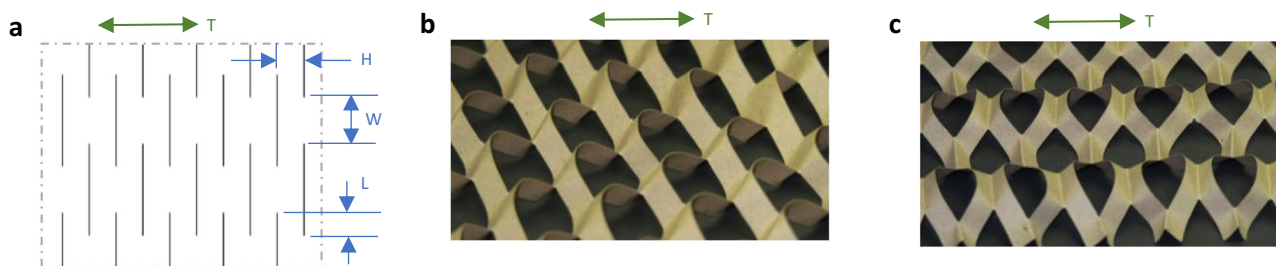
Fig. 1 Single-slit tension activated kirigami. a Schematic of the single-slit TAK pattern. **b** Deployed single-slit TAK in parallel configuration. **c** Deployed single-slit TAK in alternating configuration.
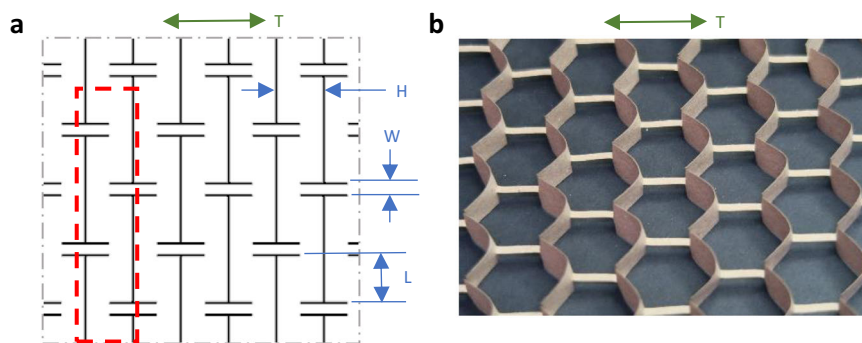
Fig. 2 Folding-wall tension activated kirigami. a Schematic of the folding-wall TAK pattern. **b** Deployed folding-wall TAK.
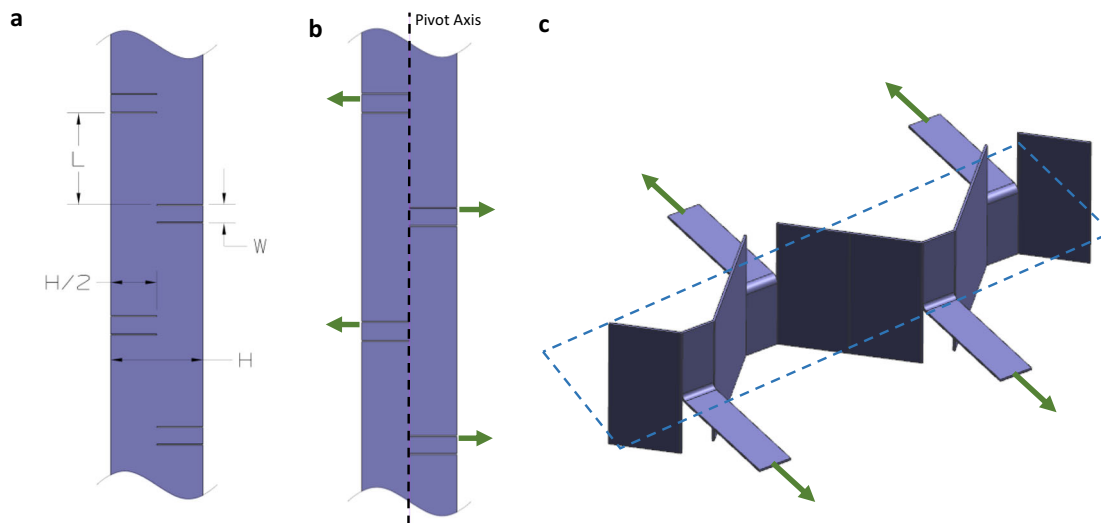
Fig. 3 Mechanics of folding-wall TAK deployment. a basic rectangular element. **b** Tension forces on the element. **c** Out-of-plane rotation and accordion folding of the element.

area occupied by the deployed structure remains quite constant (Supplementary Fig. 4).

To understand the mechanics of the Folding-Wall TAK pattern, consider a rectangular region shown by dashed lines in Fig. 2a. This region has a height of H and alternating tabs of length $H/2$ and width W spaced a distance L apart as shown in Fig. 3a. When tension is applied along axis T, the rectangular region experiences opposed forces represented by the arrows in Fig. 3b. These forces cause the region to buckle and rotate out of plane, nominally along the Pivot Axis shown in Fig. 3b. As the region rotates out of plane it also folds, creating the stable Folding-Wall structure shown in Fig. 3c. The regions directly above or below the tabs fold to become part of the continuous folded vertical wall, although if the tab width W is very small these wall sections are more curved than flat wall regions. Figure 3c shows an idealized model of the deployed Folding-Wall section where the walls are orthogonal to the original plane of the rectangle represented by the dashed rectangle. The tabs largely remain parallel to the original plane. This folded wall section resembles a portion of a standard honeycomb structure. A continuous array of these folded wall sections is created by connecting the tabs in rows of adjacent rectangular sections, as shown in the Folding-Wall TAK pattern of Fig. 2a.

It is important to note that if the material used for any TAK is too thick relative to the scale of the pattern, or if the material is too compliant, then the tension forces may not cause the material to buckle out of plane. For example, a soft foam sheet thicker than the longest slit would likely compress and deform in the original plane of the sheet and not buckle out of that plane. In addition, materials that are too weak or brittle may tear before they fully deploy. Predicting the material and geometry relationships that govern the boundary between the two responses is the subject of future work.

Strength and stiffness. A honeycomb core was chosen as the baseline of comparison for mechanical performance because of its wide use in sandwich structures. We measured the structural strength and stiffness of Folding-Wall TAK samples as well as both configurations of single-slit TAK and a constructed honeycomb using 3 different materials: paper, plastic, and aluminum. The dimensions and materials are summarized in Table 1.

The TAK samples created using paper and plastic retracted when tension was released. To allow for consistent testing conditions, we placed the samples on a 12.7 mm thick aluminum plate and taped the ends holding them in the deployed state. The forces introduced by the tape could not be easily measured and were not accounted for in the analysis.

Six samples were created for each of the twelve scenarios in Fig. 4. We placed the aluminum plate with each sample in a load frame and compressed the sample with a custom aluminum circular platen of diameter 100 mm. Force and displacement were measured versus time for each sample and converted to stress and strain. Figure 5 shows typical stress vs. strain curves collected for the constructions made of aluminum. The folding-wall TAK and constructed honeycomb samples show a well-defined elastic

Table 1 Sample materials and dimensions.

Sample Type	Single-slit TAK (parallel and alternating)	Fig. 1A; L = 5.4 mm, H = 5.4 mm, W = 10.8 mm; extended +33%
	Folding-Wall TAK	Fig. 3A; L = 5.8 mm, H = 5.8 mm, W = 1.2 mm; extended +50%
	Constructed Honeycomb	22 strips (12 mm wide), folded every 12 mm, attached with adhesive into regular hexagon pattern covering more than 200 × 200 mm.
Materials	Paper	0.113 mm thick virgin paper
	Plastic	0.081 mm thick green polyester film
	Aluminum	0.077 mm thick 3003-alloy foil
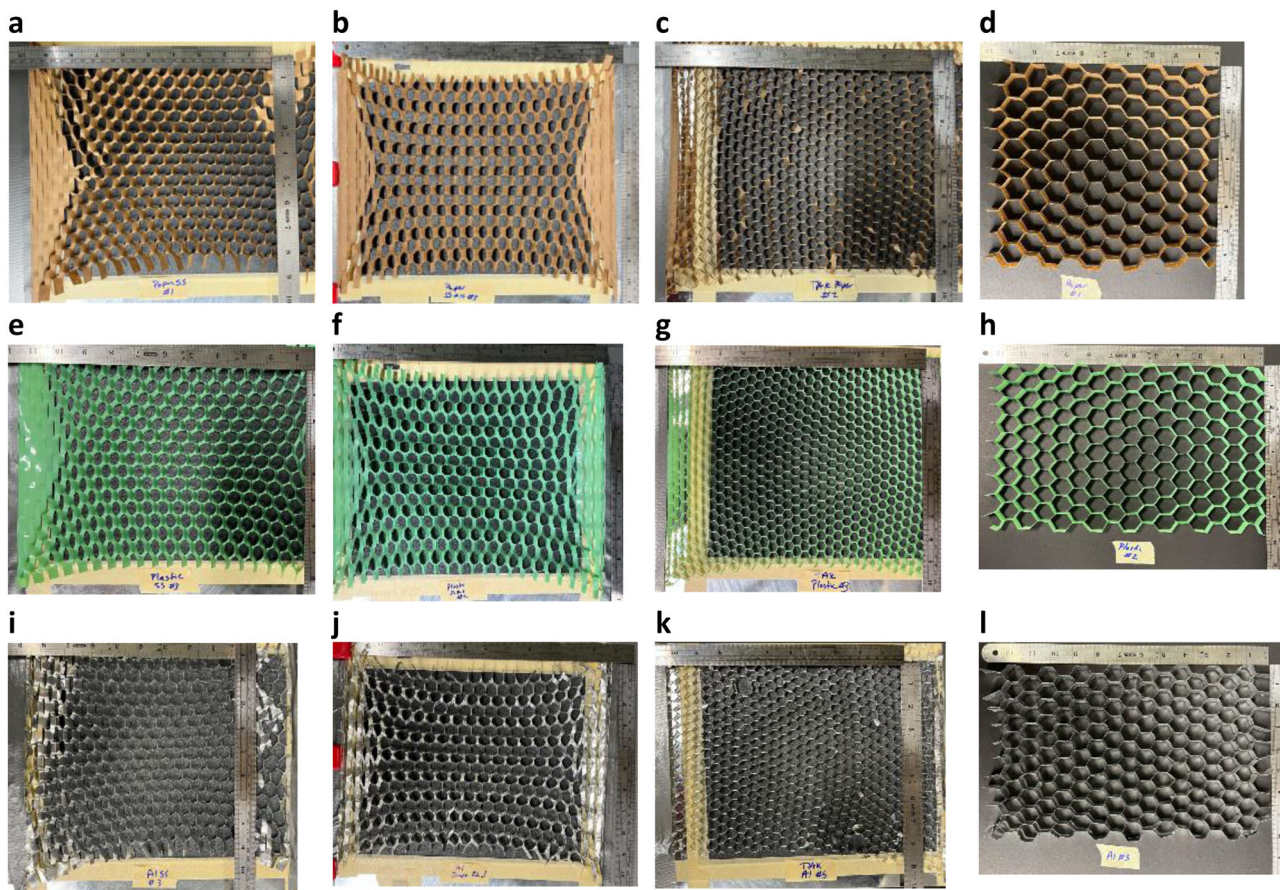
Fig. 4 Samples prepared for compression testing. a Single-slit TAK—parallel (paper). **b** Single-slit TAK—alternating (paper). **c** Folding-wall TAK (paper). **d** Constructed honeycomb (paper). **e** Single-slit TAK—parallel (plastic). **f** Single-slit TAK—alternating (plastic). **g** Folding-wall TAK (plastic). **h** Constructed honeycomb (plastic). **i** Single-slit TAK—parallel (aluminum). **j** Single-slit TAK—alternating (aluminum). **k** Folding-wall TAK (aluminum). **l** Constructed honeycomb (aluminum).
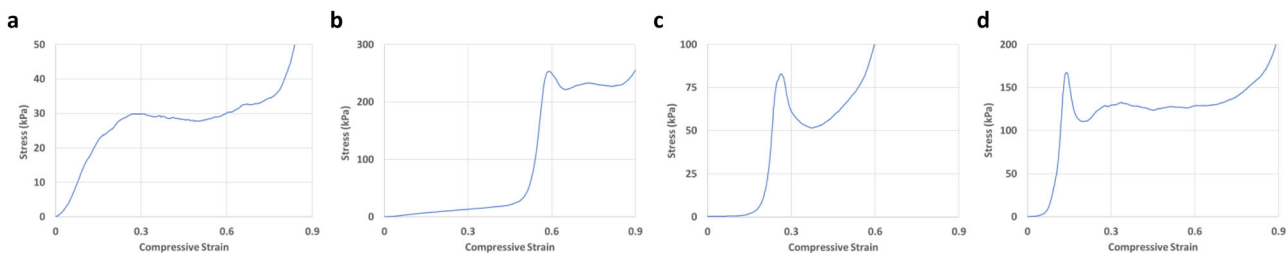
Fig. 5 Typical stress-strain curves from compressed samples. a Single-slit TAK, parallel (Al). **b** Single-slit TAK, alternating (Al). **c** Folding-wall TAK (Al). **d** Constructed Honeycomb (Al).

region with a peak force before the initial onset of buckling. The parallel single-slit TAK pattern had a less defined peak force that became hard to identify in the paper samples. The alternating single-slit TAK pattern showed a less stiff linear region up to around 50% strain where it settled into a stronger configuration with a much stiffer linear region and a peak. Because this peak occurred after a second linear region it may not be directly comparable to the peak stiffnesses in the other samples but is certainly an intriguing characteristic of the pattern. The general shape of the plots was consistent across all three materials: paper, plastic, and aluminum (Supplementary Figs. 6–8).

The slope of the stress-strain curve was estimated to find the elastic modulus, or stiffness of each sample. We also measured the thickness of the deployed samples, or the loft, from the curves (Supplementary Note 2) and combined with geometric calculations to estimate the density of the sample in the deployed state (Supplementary Notes 1 and 3). The elastic modulus, or stiffness, was divided by the density to produce a specific stiffness. The peak stress (a.k.a. strength) before buckling was also extracted from the curves. This strength was divided by the density to produce a specific strength. The averages and standard deviations for each of the types of sample are summarized in Table 2.

These results show that single-slit TAK structures deployed in the alternating configuration are initially less stiff than all configurations with a second stiffer region and peak after significant strain. They also show that folding-wall TAK structures are significantly stiffer and stronger than either of the single-slit TAK configurations in the initial 30% strain regions. Although the folding-wall TAK samples are shown to be weaker than the constructed honeycomb samples, the difference is less significant when the amount of material is considered as shown by the specific stiffness and specific strength. We conclude from this data that the Folding-Wall TAK samples create useful honeycomb-like structures with superior strength compared to single-slit TAK samples. They may also be useful replacements for some full honeycomb structures, eliminating the need for folding, arranging strips, and bonding adjacent rows while also providing high conformability that enables use in non-planar applications.

Volume expansion and energy absorption. In addition to strength or stiffness of individual layers, we found other advantages of the TAK structures compared to a full honeycomb structure. The TAK samples deploy to occupy space and can absorb energy when subsequently compressed. They also conform easily around objects, unlike honeycomb or origami structures. These characteristics make them good candidates for use as an expanding cushioning wrap.

We laser cut single-slit and Folding-Wall TAK patterns into long sheets of paper, extended them, and wrapped them around a thin, flat frame producing the samples shown in Fig. 6. Six wrapped samples were made of each type. Details are summarized in Table 3. The single-slit dimensions were chosen to match several commercially available paper-wraps first developed in the 1990's[37].

We found that adjacent layers of the Folding-Wall TAK interlocked when wrapped around an object or itself, holding the pad in its final shape while being handled. The single-slit TAK naturally deployed into the parallel configuration then tended to unwrap, so we applied tape to hold the pad in its wrapped shape. We learned that the single-slit pattern took significantly more force to extend than the Folding-Wall TAK. All pads of material were compressed between a flat plate and a 76.2 mm diameter platen in a load frame at 1 mm per second to a maximum force of 8896 N. We recorded the resistance force and displacement during compression. The total loft of wrapped layers was defined as the distance traveled from first detecting resistance until a maximum force of 4448 N was reached. The total energy absorbed by the pad was calculated by integrating the force vs distance curve from the onset of resistance to 4448 N. The results are summarized in Table 4 (Supplementary Fig. 9).

Both the TAK patterns became narrower when extended, so their area changes with strain. To calculate the total volume change when expanded, we used a geometric analysis to calculate the Area Expansion Ratio, or the ratio of the deployed area to the
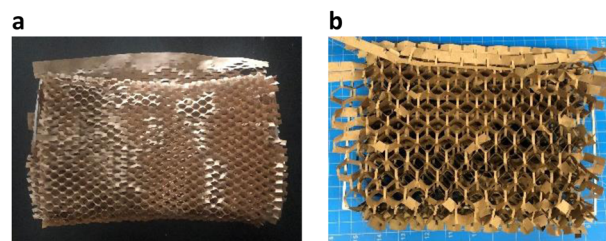
Fig. 6 Long paper samples wrapped for compression testing. a Single-slit TAK. **b** Folding-wall TAK.

Table 2 Stiffness and strength measurements for compressed samples.

|	Fig.	Description	Density [mg cm^{-3}]	Stiffness [kPa]		Specific Stiffness [N m kg^{-1}]		Strength [kPa]		Specific Strength [N m kg^{-1}]	
				Ave	StDev	Ave	StDev	Ave	StDev	Ave	StDev
Paper	4a	single-slit TAK, parallel	12.9	72	6	5615	493	8.3	2	645	141
	4b	single-slit TAK, alternating	13.3	25	0	1847	36	44*	3	3279*	188
	4c	Folding-Wall TAK	12.6	428	72	34,005	5755	27	1	2152	104
	4d	Constructed Honeycomb	14.9	733	67	49,278	4532	29	1	1961	69
Plastic	4e	single-slit TAK, parallel	20.5	118	9	5745	442	15	1	732	33
	4f	single-slit TAK, alternating	21.4	65	8	3020	353	90*	6	4211*	291
	4g	Folding-Wall TAK	21.0	692	118	32,925	5597	60	9	2839	419
	4h	Constructed Honeycomb	24.9	2159	164	86,855	6592	78	4	3144	151
Aluminum	4i	single-slit TAK, parallel	40.4	186	25	4612	616	30	2	746	40
	4j	single-slit TAK, alternating	40.9	45	4	1091	98	236*	18	5780*	444
	4k	Folding-Wall TAK	41.0	1289	353	31,415	8612	75	5	1833	115
	4l	Constructed Honeycomb	47.5	5154	603	108,516	12,698	167	7	3525	151

Asterix shows that late peak strength values are reported for the alternating configurations.

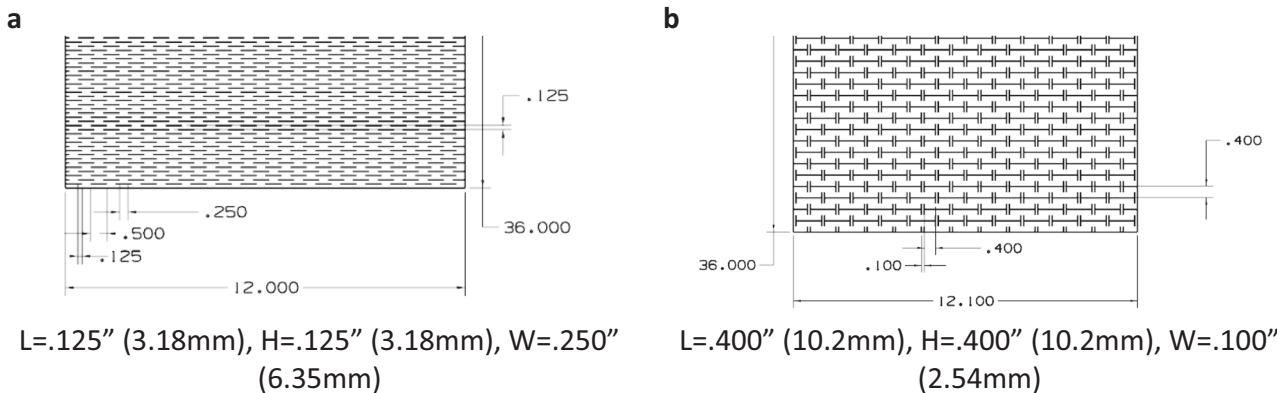**Table 3 Volume expansion and energy absorption test materials and dimensions.**

		Ref Figure & Pattern Dimensions	Overall Dimensions	Extension	layers	Material
Sample Type	Single-slit TAK	Fig. 1A; L = 3.18 mm, H = 3.18 mm, W = 6.35 mm	305 × 914 mm	+33%	7	0.19 mm thick recycled kraft paper
	Folding-Wall TAK	Fig. 3A; L = 10.2 mm, H = 10.2 mm, W = 2.54 mm	307 × 914 mm	+50%	8	

Table 4 Volume expansion and energy absorption results.

Sample	Energy Absorbed per Layer [J]	Loft per Layer [mm]	Volume Expansion Ratio
Single-Slit TAK	0.42	4.4	25.4
Folding-Wall TAK	0.59	7.9	55.5

a

L=.21" (5.4mm), H=.21" (5.4mm), W=.43" (10.8mm)

b

L=.23" (5.8mm), H=.23" (5.8mm), W=.05" (1.2mm)
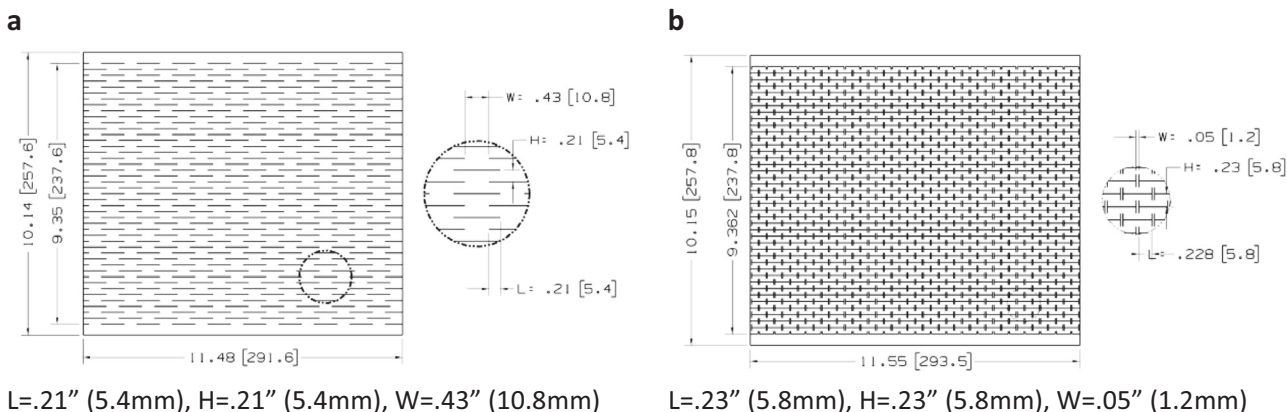
Fig. 7 Structural strength testing patterns. a Single-slit pattern. **b** Folding-wall pattern.

a

L=.125" (3.18mm), H=.125" (3.18mm), W=.250" (6.35mm)

b

L=.400" (10.2mm), H=.400" (10.2mm), W=.100" (2.54mm)

Fig. 8 Volume expansion and energy absorption testing patterns. a Single-slit pattern. **b** Folding-wall pattern.

area of flat, undeployed material required to fill that area (Supplementary Note 1). This Area Expansion Ratio is multiplied by the loft per layer to find the volume expansion ratio for the two samples, where $\text{VolumeExpansionRatio} = \frac{\text{Volume}_{\text{deployed}}}{\text{Volume}_{\text{flat}}}$ (Supplementary Note 4).

The results show that the Folding-Wall TAK is superior to the single-slit TAK in terms of energy absorption and volumetric expansion, suggesting that it might comprise an improved sustainable cushioning product. The strong interlocking of adjacent layers adds additional value to the Folding-Wall TAK since in a wrapped form it does not require a tape or adhesive to hold its shape.

Conclusions

We have introduced a kirigami pattern that can be activated by tension into a deployed state with large folded wall regions that are orthogonal to the original plane of the sheet. The resulting structure is strong and stiff; with a specific strength and specific stiffness averaging 84% and 45% respectively of a full honeycomb construction of the same density across three material sets. It also expands to occupy much greater volume in the deployed state, absorbs energy when compressed, and is very easy to deploy. In addition, we found that multiple layers of this pattern interlock with each other. The combination of these features suggests that the Folding-Wall Tension Activated Kirigami could have significant value for many applications.
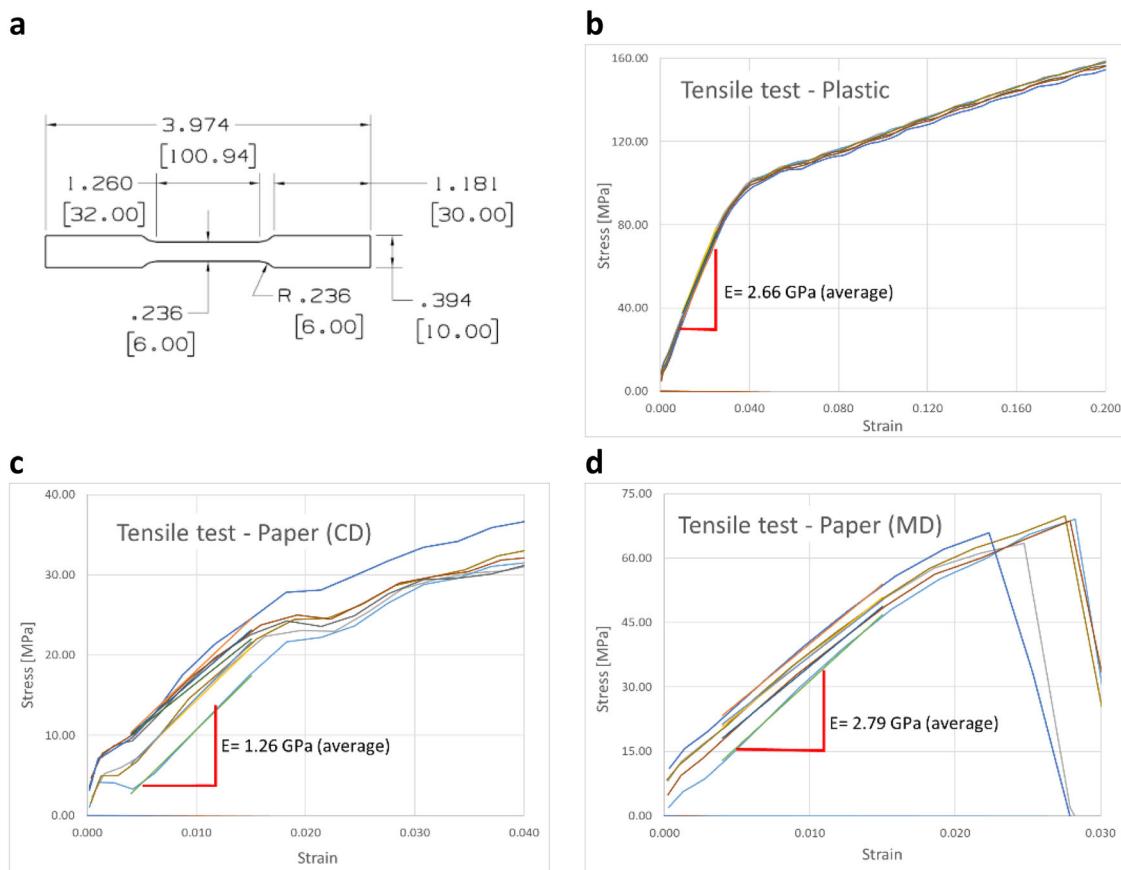
Fig. 9 Tensile testing of material samples. a test sample dimensions. **b** Stress-strain curves for plastic samples. **c** Stress-strain curves for paper samples, pulled in the cross direction. **d** Stress-strain curves for paper samples, pulled in the machine direction.

Methods

Fabricating samples. We cut paper and plastic samples into respective substrates using a Model XLS 10.150D laser cutter (obtained from Universal Laser Systems, Inc., Scottsdale, AZ). Aluminum samples were formed using a Mitsubishi Fiber Optic Laser: ML 3015 eX-F40 with the EX-F M800/LC30EF Control.

Patterns. The patterns shown in Fig. 7 were used to produce the testing samples of Fig. 4, with results shown in Table 2. For the paper samples, Virgin paper was used as described below.

The patterns shown in Fig. 8 were used for the roll testing shown in Fig. 6 with subsequent results in Table 4. These samples were created using Kraft Paper as described below.

Materials. The following materials were used in this work.

Kraft paper. brown kraft paper from Uline, Pleasant Prairie, WI under trade designation "S-7051". It is 100% recycled paper and has a thickness of about 0.0075" (0.19 mm) when measured according to test method TAPPI T411 om-10. The basis weight was measured as 126.5 grams per square meter according to test method TAPPI T410 om-13. The density can be calculated as the basis weight divided by the caliper = 0.666 g/cm^3.

Virgin paper. Brown virgin paper from Uline, Pleasant Prairie, WI under trade designation "S-20806". It has a thickness of 0.113 mm when measured according to test method TAPPI T411 om-10. The basis weight was measured as 67.5 grams per square meter according to test method TAPPI T410 om-13. The density can be calculated as the basis weight divided by the caliper = 0.599 g/cm^3.

Plastic. 3 mil polyester from McMaster Carr PN: 9513K146. It has a thickness of 0.081 mm when measured according to test method TAPPI T411 om-10. The basis weight was measured as 111.3 grams per square meter according to test method TAPPI T410 om-13. The density can be calculated as the basis weight divided by the caliper = 1.37 g/cm^3.

Aluminum. Corrosion-Resistant 3003 Aluminum Sheets, .003" thick, obtained from McMaster Carr PN:3970N12. Certification specified thickness = 0.00304" (0.077 mm), Tensile Strength = 15,803 psi (108.96 MPa), Yield Strength = 7417 psi (51.14 MPa). Material standards report typical density as 2.73 g/cm^3.

Additional mechanical properties for some of the material sets were obtained by laser cutting test specimens according to ASTM-E8 M-04 and tensile testing them on the MTS load frame described below. The stress strain curves for the samples are shown in Fig. 9. Multiple samples are overlaid in the stress-strain plots, but the slope (Young's Modulus) is reported as an average of all the samples.

Test preparation. The following procedures were used to prepare the different samples for testing.

1. Single Slit Tension Activated Kirigami
   We prepared single slit TAK samples by taping one end of the sample to one edge of an aluminum plate (0.5" thick, 12" × 16"). The sample was then stretched to the target length of 133% (the 9.35" dimension extended to 12.5"), and a single sheet of 9" × 11" 3 M Wetordry^{TM} 100 grit sandpaper [431Q] was placed underneath the sample to avoid slipping during compressions. A 100 mm diameter piece of the sandpaper was also fastened to the top platen.
   Although the target was 133% extension, the first several rows on each side could not fully extend, as can be seen in Fig. 4. Because of this, the material being tested at the center of the sample was extended more than the target, reaching the maximum possible extension. The extension was measured from the images and used in the calculations instead of the original target. Using the laser cut samples and plate described, the edge of the sample was placed ½" (12 mm) from the edge of the plate and taped down with a strip of tape covering the full width of the sample. The sample was then deployed and expanded to the target length and taped down with another strip of tape covering the full width of the sample. For all samples, 3M Scotch Duct Tape [920-P-GRN-C] was used to secure the sample. For aluminum samples, no adhesive was needed to secure the samples as the aluminum held its shape after deployment.
   We used a ruler to deploy the single slit pattern in the parallel alignment. While one hand pulled the edge of the sample to expand it at a slight
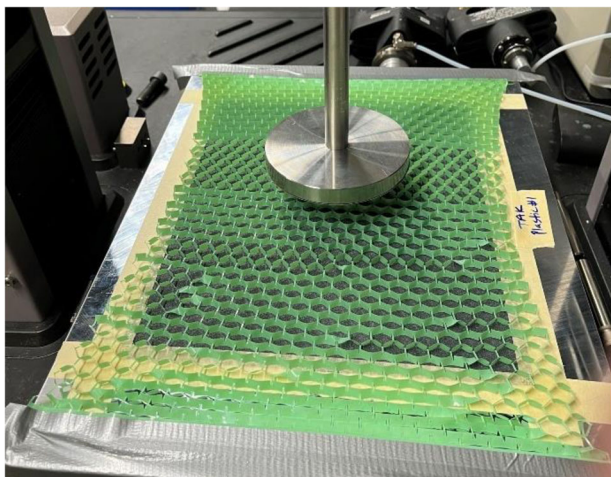
Fig. 10 Compression testing. A typical test specimen is shown just before compression testing.

upwards angle from the plate, the other hand applied light pressure to the undeployed section of the sample to ensure an even and parallel deployment. To deploy the single slit pattern in the alternating alignment, the sample was gently folded prior to deployment. This fold is made by folding each 5.4 mm (0.21") segment on top of one another, alternating direction like an accordion. At each level, we made a gentle crease to train each segment to deploy in the correct direction. The occasional region may invert despite folding but can be fixed by hand once the sample is fully deployed and taped down.

2. Folding-Wall Tension Activated Kirigami

We prepared Folding-Wall TAK samples by taping one end of the sample to one edge of an aluminum plate (0.5" thick, 12" × 16"). The sample was then stretched the to the target length of 150% (the 9.36" dimension extended to 14"), and a single sheet of 9" × 11" 3 M Wetordry™ 100 grit sandpaper [431Q] was placed underneath the sample to avoid slipping during compressions. A 100 mm diameter piece of the sandpaper was also fastened to the top platen.

Although the target was 150% extension, the first few rows on each side could not fully extend, as can be seen in Fig. 4. Because of this, the material being tested at the center of the sample was extended more than the target. The extension was measured from the images and used in the calculations instead of the original target.

Using the laser cut samples and plate described, the edge of the sample was placed ½" (12 mm) from the edge of the plate and taped down with a strip of tape to cover the complete end of the sample. The sample was then deployed and expanded to the target length and taped down with another strip of tape to cover the complete end of the sample. For all samples, 3 M Scotch Duct Tape [920-P-GRN-C] was used to secure the sample. For aluminum samples, no adhesive was needed to secure the samples as the aluminum held its shape upon deployment.

We extended the folding wall samples from the secured end. Prior to extension, the free end of the sample was also taped down for easier taping of the second edge. Usually, there are singular segments that need to be flipped individually, but each row should all go the same direction and will be near perpendicular to the plate at full extension.

3. Constructed Honeycomb

The constructed honeycomb samples consist of 22 strips (12 × 384 mm) which are stuck together using Scotch ATG Adhesive Transfer Tape [924]. We used a jig to individually fold these strips with 32 consecutive 60-degree bends that are all 12 mm apart and form half-hexagons. The folds used to make these bends alternate every two folding locations which gives the hexagon shape.

After all strips were folded, they were stuck together with pieces of transfer tape to form a honeycomb structure. To aide in accurate testing, the adhesion of these strips was done carefully making sure the strips were completely fastened together all at the same height, flush with the tabletop, and aligned properly for a complete honeycomb structure.

Compression. The compression testing was carried out using an MTS load frame [MTS Criterion Model C43 104E, from Mechanical Testing Systems Corporation, Eden Prairie, MN]. We placed the test samples on a bottom platen large enough to hold the sample and the sample was compressed from the top using a custom made 100 mm diameter foot (Fig. 10). The compression speed was 1.0 mm/s and the maximum force was 2000 lbs [8900 N]; the data was trimmed at 1000 lbs [4448 N].

Force vs. displacement information along with the time stamp for each data point at a rate of 100 data points per second was recorded.

Data availability
The datasets generated or analyzed during the current study are available from the corresponding author on reasonable request.

Code availability
The code generated during the current study is available from the corresponding author on reasonable request.

References
1. Callens, S. J. P. & Zadpoor, A. A. From flat sheets to curved geometries: origami and kirigami approaches. *Mater. Today* **21**, 241–264 (2018).
2. Mahadevan, L. & Rica, S. Self-organized origami. *Science* **307**, 1740 (2005).
3. Demaine, E. D. & Tachi, T. Origamizer: a practical algorithm for folding any polyhedron. In *Proc. 33rd International Symposium on Computational Geometry (SoCG 2017)* **34**:1–34:15 (2017).
4. Del Grosso, A. & Basso, P. Adaptive building skin structures. *Smart Mater. Struct.* **19**, 124011 (2010).
5. Seymour, K. et al. Origami-based deployable ballistic barrier. In *Proc. 7th International Meeting on Origami in Science Mathematics and Education* 763–778 (2018).
6. Melancon, D., Gorissen, B., García-Mora, C. J., Hoberman, C. & Bertoldi, K. Multistable inflatable origami structures at the metre scale. *Nature.* **592**, 545–550 (2021).
7. Rus, D. & Tolley, M. T. Design, fabrication and control of origami robots. *Nat. Rev. Mater.* **3**, 101–112 (2018).
8. Yang, L. V. et al. On the out-of-plane compression of a Miura-ori patterned sheet. *Int. J. Mech. Sci.* **161–162**, 105022 (2019).
9. Demaine, E. D., Demaine, M. L., Koschitz, D. & Tachi, T. Curved crease folding—a review on art, design and mathematics. In *Proc IABSE-IASS Symposium: Taller, Longer, Lighter* (IABSE-IASS2011), London, England, 20–23 (2011).
10. Woodruff, S. R. & Filipov, E. T. Curved creases redistribute global bending stiffness in corrugations: theory and experimentation. *Meccanica* **56**, 1613–1634 (2021).
11. Park, J. J., Won, P. & Ko, S. H. A review on hierarchical origami and kirigami structure for engineering applications. *Int. J. Precis. Eng. Manuf.-Green Tech.* **6**, 147–161 (2019).
12. Castle, T. et al. Making the cut: lattice kirigami rules. *Phys. Rev. Lett.* **113**, 245502 (2014).
13. Castle, T., Sussman, D., Tanis, M. & Kamien, R. D. Additive lattice kirigami. *Sci. Adv.* **23**, e1601258 (2016).
14. Chen, B. G. et al. Topological mechanics of origami and kirigami. *Phys. Rev. Lett.* **116**, 135501 (2016).
15. Seffen, K. K-Cones and kirigami metamaterials. *Phys. Rev. E* **94**, 033003 (2016).
16. Tang, Y. & Yin, J. Design of cut unit geometry in hierarchical kirigami-based auxetic metamaterials for high stretchability and compressibility. *Extreme Mech. Lett.* **12**, 77–85 (2017).
17. Yang, C. et al. Kirigami-inspired deformable 3D structures conformable to curved biological surface. *Adv. Sci.* **5**, 1801070 (2018).
18. Cho, Y. et al. Engineering the shape and structure of materials by fractal cut. *Proc. Natl Acad. Sci.* **111**, 17390–17395 (2014).
19. Choi, G. P. T., Dudte, L. H. & Mahadevan, L. Programming shape using kirigami tessellations. *Nat. Mater.* **18**, 999–1004 (2019).
20. Coulais, C., Sabbadini, A., Vink, F. & van Hecke, M. Multi-step self-guided pathways for shape-changing metamaterials. *Nature* **561**, 512–515 (2018).
21. An, N., Domel, A. G., Zhou, J., Rafsanjani, A. & Bertoldi, K. Programmable heirarchical kirigami. *Adv. Funct. Mater.* **30.6**, 1906711 (2020).
22. Rafsanjani, A. & Bertoldi, K. Buckling-induced kirigami. *Phys. Rev. Lett.* **118**, 084301 (2017).
23. Yan, Z. et al. Controlled mechanical buckling for origami-inspired construction of 3D microstructures in advanced materials. *Adv. Funct. Mater.* **26**, 2629 (2016).
24. Zhang, Y. et al. Kirigami-inspired 3D mesostructures in membranes. *Proc. Natl Acad. Sci.* **112**, 11757–11764 (2015).
25. Elsayed, E. & Basily, B. A continuous folding process for sheet materials. *Int. Journal of Materials and Product Tech.* **21**, 217–238 (2004).

26. Wang, Y. & Wang, C. Buckling of ultrastretchable kirigami metastructures for mechanical programmability and energy harvesting. *Int. J Solids Struct.* **213**, 93–102 (2021).

27. Rafsanjani, A., Jin, L., Deng, B. & Bertoldi, K. Propagation of pop ups in kirigami shells. *Proc. Natl Acad. Sci. USA* **116**, 8200–8205 (2019).

28. Lamoureux, A., Lee, K., Shlian, M., Forrest, S. R. & Shtein, M. Dynamic kirigami structures for integrated solar tracking. *Nat. Commun.* **6**, 8092 (2015).

29. Babaee, S. et al. Bioinspired kirigami metasurfaces as assistive shoe grips. *Nat. Biomed. Eng.* **4**, 778–786 (2020).

30. Abhinav, S. N. & Budharaju, M. V. A review paper on origin of honeycomb structure and its sailing properties. *Int. J. Engineer Res. Technol.* **9.8**, 861–866 (2020).

31. Dean, H. B. Artificial honeycomb. US patent 1,389,294 (1921).

32. Saito, K., Pellegrino, S. & Nojima, T. Manufacture of arbitrary cross-section composite honeycomb cores based on origami techniques. *J. Mech. Des.* **136**, 051011 (2014).

33. Bauer, J. et al. "Nanolattices: an emerging class of mechanical metamaterials.". *Adv. Mater.* **29.40**, 1701850 (2017).

34. Zhang, Q. et al. Bioinspired engineering of honeycomb structure—using nature to inspire human innovation. *Prog. Mater. Sci.* **74**, 332–400 (2015).

35. Neville, R., Scarpa, F. & Pirrera, A. Shape morphing kirigami mechanical metamaterials. *Sci. Rep.* **6**, 31067 (2016).

36. Scotch Cushion Lock Protective Wrap, www.scotchbrand.com/cushionlock, Accessed 9 Jan (2023)

37. Goodrich, D. P. & Hurwitz, M. C. Slit sheet packing material. US patent 5,667,871 (1997).

Acknowledgements

Author contributions

T.C. conceived the presented idea and drafted the manuscript. T.C., D.L.-A. and P.F. discussed results and revised the manuscript. D.L.-A. collected data for the Strength and Stiffness section. C.E. prepared samples and collected data for the Volume Expansion and Energy Absorption section and contributed to the Methods section. T.C. performed the computations, analysis, and prepared graphs with input from D.L.-A. and P.F.

Competing interests

All authors were employees of 3 M Company when contributions were made. T.C., P.F. and D.L.-A. are co-inventors on the following US patent applications (3 M Innovative Properties is the assignee): US20220380107A1 Tension-activated, expanding sheets; US20230020226A1 Tension-activated, expanding sheets with compound slits; US20230022987A1 Single slit patterned, tension-activated, expanding articles. T.C is inventor on US design patent US-D971019-S Extended Sheet (3 M Innovative Properties is the assignee).

Additional information

Supplementary information The online version contains supplementary material available at https://doi.org/10.1038/s43246-023-00357-4.

Correspondence and requests for materials should be addressed to Tom Corrigan.

Peer review information *Communications Materials* thanks the anonymous reviewers for their contribution to the peer review of this work. Primary Handling Editor: Aldo Isidori. Peer reviewer reports are available.

Reprints and permission information is available at http://www.nature.com/reprints

Publisher's note Springer Nature remains neutral with regard to jurisdictional claims in published maps and institutional affiliations.